

## Development of a quasi-monoenergetic 6 MeV Gamma Facility at NASA Goddard Space Flight Center

Suzanne F. Nowicki<sup>a,b,c,\*</sup>, Stanley D. Hunter<sup>c</sup>, Ann M. Parsons<sup>c</sup>

<sup>a</sup> University Space Research Association, Columbia, MD 21044, USA

<sup>b</sup> University of Michigan, Applied Physics, Ann Arbor, MI 48109, USA

<sup>c</sup> NASA Goddard Space Flight Center, Greenbelt, MD 20771, USA

### ARTICLE INFO

#### Article history:

Received 2 October 2012

Received in revised form

5 December 2012

Accepted 6 December 2012

Available online 14 December 2012

#### Keywords:

6.129 MeV

Monoenergetic

Facility

Characterization

Calibration

Gamma-ray

Neutron

Pulsed neutron generator

### ABSTRACT

The 6 MeV Gamma Facility has been developed at NASA Goddard Space Flight Center (GSFC) to allow in-house characterization and testing of a wide range of gamma-ray instruments such as pixelated CdZnTe detectors for planetary science and Compton and pair-production imaging telescopes for astrophysics. The 6 MeV Gamma Facility utilizes a circulating flow of water irradiated by 14 MeV neutrons to produce gamma rays via neutron capture on oxygen ( $^{16}\text{O}(\text{n},\text{p})^{16}\text{N} \rightarrow ^{16}\text{O}^* \rightarrow ^{16}\text{O} + \gamma$ ). The facility provides a low cost, in-house source of 2.742, 6.129 and 7.117 MeV gamma rays, near the lower energy range of most accelerators and well above the 2.614 MeV line from the  $^{228}\text{Th}$  decay chain, the highest energy gamma ray available from a natural radionuclide. The 7.13 s half-life of the  $^{16}\text{N}$  decay allows the water to be irradiated on one side of a large granite block and pumped to the opposite side to decay. Separating the irradiation and decay regions allows for shielding material, the granite block, to be placed between them, thus reducing the low-energy gamma-ray continuum. Comparison between high purity germanium (HPGe) spectra from the facility and a manufactured source,  $^{238}\text{Pu}/^{13}\text{C}$ , shows that the low-energy continuum from the facility is reduced by a factor  $\sim 30$  and the gamma-ray rate is  $\sim 100$  times higher at 6.129 MeV.

© 2012 Elsevier B.V. All rights reserved.

### 1. Introduction

Development of gamma-ray spectrometers and imaging telescopes for planetary science and medium-energy gamma-ray astrophysics requires characterization, optimization, and ultimately pre-flight calibration. Characterization and optimization can be readily accomplished using natural radioactive sources; however, the highest gamma-ray energy available from a natural radionuclide is the 2.614 MeV line from the  $^{228}\text{Th}$  decay chain. Higher energy, collimated, and polarized gamma-ray beams are readily available at accelerators, such as the Triangle University Nuclear Laboratory High Intensity Gamma-Ray Source (HIGS) at the Duke Free Electron Laser Laboratory (DFELL). These facilities provide ideal environments for instrument pre-flight calibration; however, the cost and logistics associated with accelerator tests preclude their common use for instrument characterization and optimization. The 6 MeV Gamma Facility has been developed at NASA/GSFC to provide a in-house, low background source of monoenergetic, 2.742, 6.129, and 7.117 MeV, gamma rays

generated via the  $^{16}\text{O}(\text{n},\text{p})^{16}\text{N} \rightarrow ^{16}\text{O}^* \rightarrow ^{16}\text{O} + \gamma$  reaction. These gamma rays are also available from manufactured sources, such as  $^{238}\text{Pu} + ^{13}\text{C}$  ( $\alpha + ^{13}\text{C} \rightarrow ^{17}\text{O} \rightarrow ^{16}\text{O}^* \rightarrow ^{16}\text{O} + \gamma$ ); however, the low-energy gamma-ray and neutron emissions from these sources decrease the relative intensity of 6 MeV gamma rays. A  $^{238}\text{Pu}/^{13}\text{C}$  source with 6.129 MeV gamma-ray rate comparable to that of the NASA/GSFC Gamma Facility would have a total activity of  $\sim 43$  Ci, far too strong a source for safe laboratory use.

Systems such as the one developed by Kroupa et al. [1] also provide monoenergetic gamma-ray lines above 3 MeV but such systems do not provide shielding against low-energy gamma rays, such as the 2.2 MeV line from neutron capture on hydrogen. By shielding these other lines, significant reduction in Compton continuum can be observed compared to manufactured sources such as  $^{238}\text{Pu}/^{13}\text{C}$ .

The 6 MeV Gamma Facility adds additional in-house instrument development capabilities to the unique planetary sciences test facility developed at Goddard Geophysical and Astronomical Observatory (GGAO) [2]. These capabilities include characterization, optimization, and calibration of instruments such as pixelated CdZnTe detectors [3] and  $\text{SrI}_2$  scintillators [4] at the upper end of their energy range, and the AdEPT pair telescope at the difficult low end of its energy range [5]. The GGAO is a unique outdoor facility that allows remote operation of a Thermo MP320

\* Corresponding author at: NASA Goddard Space Flight Center 8800 Greenbelt Rd, Bldg 34, room W271 Greenbelt, MD 20771 United States.  
Tel./fax: +1 301 614 7034.

E-mail address: [suzanne.f.nowicki@nasa.gov](mailto:suzanne.f.nowicki@nasa.gov) (S.F. Nowicki).

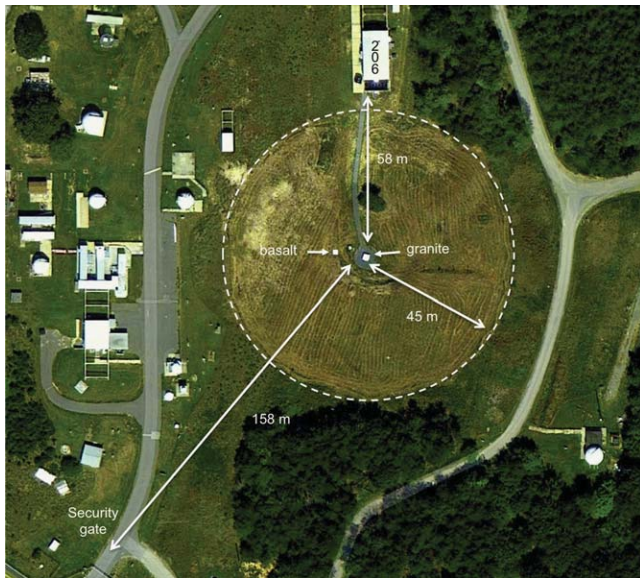


**Fig. 1.** Aerial view of the GSFC/GGAO test site showing the 45 m radius safety perimeter (white dashed circle) defined by the GSFC Radiation Safety Office. The remote operation building (Building 206) is shown at the top of the image. The granite block supporting the 6 MeV Gamma Facility is located at the center of the safety perimeter and the basalt block is nearby to the left.

D–T pulsed neutron generator (PNG) for calibration of neutron/gamma-ray instrumentation for planetary science applications. Two large, 1.8 m × 1.8 m × 0.9 m, blocks of granite and basalt, visible in the aerial view of the GGAO site shown in Fig. 1, provide standards for elemental composition measurements for the development of planetary science instrumentation [6].

## 2. Facility design

### 2.1. Concept

Gamma rays are generated via the  $^{16}\text{O}(n,p)^{16}\text{N}$  reaction using the 14 MeV neutrons from the PNG to activate oxygen in a volume of water continuously circulated around the granite block. The cross-section for the  $^{16}\text{O}(n,p)^{16}\text{N}$  reaction is  $4.2 \times 10^{-2}$  b at 14 MeV [7]. The  $^{16}\text{N}$  decays via beta decay, as seen in Fig. 2, with a 7.13 s half-life [7] to an excited state of  $^{16}\text{O}^*$  that rapidly de-excites producing gamma rays with energies of 2.742, 6.129, and 7.117 MeV, with emission probabilities of 0.82%, 67%, and 4.9%, respectively, and no gamma ray produced 28% of the time [7].

The 7.13 s half-life of the  $^{16}\text{N}$  decay to  $^{16}\text{O}$  allows the water to be irradiated on one side of the granite block and then transported to the gamma emission loop on the opposite side of the block shown schematically in Fig. 3(a). The 1.8 m thick granite block provides shielding from most of the neutrons and protons generated by the PNG and the  $^{16}\text{O}(n,p)^{16}\text{N}$  reaction as well as gamma rays produced by other prompt neutron reactions in the granite and soil elements. Similar approaches were used by Bishop [8] by circulating the cooling water from a reactor and by Nishitani et al. [9], who used activation of circulating water as a fusion power monitor.

The 6 MeV Gamma Facility, as shown in Fig. 3(b), consists of a closed loop of polyvinyl chloride (PVC) pipe supported by a steel framework resting on the granite block. The closed loop has two major components: the ‘neutron activation loop’ and the ‘gamma emission loop’. The input and output of the activation and decay loops are connected by the ‘supply pipe’ and the ‘return pipe’. The return pipe contains an in-line circulation pump, TACO Model 2400-50, and a flow rate meter, Omega Model FTB-1307. PVC pipe

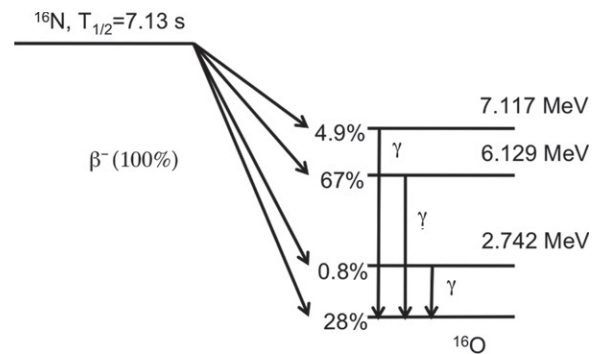


**Fig. 2.**  $^{16}\text{N}$  beta decay level scheme [7].

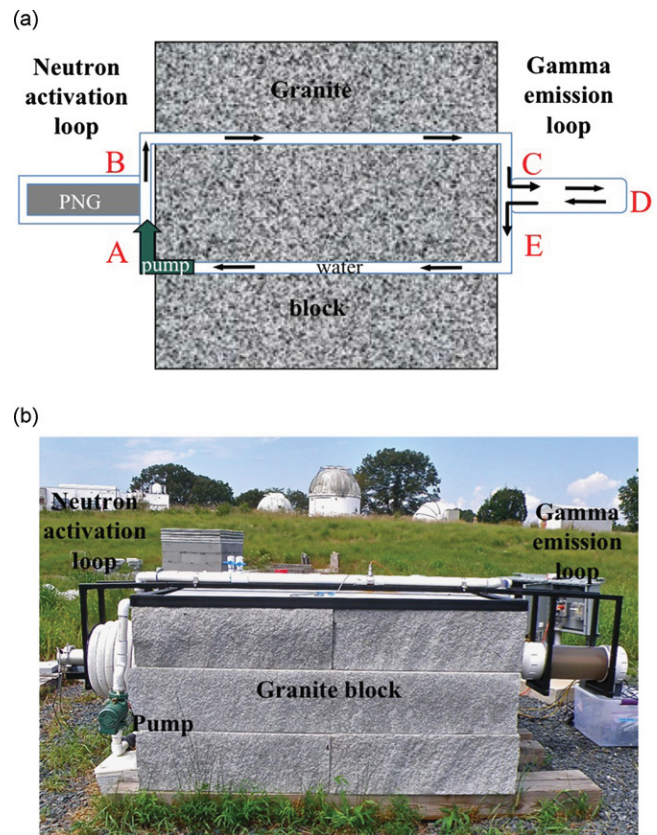


**Fig. 3.** Schematic, top view (a) and side view picture (b) of the 6 MeV Gamma Facility. The closed loop of PVC pipe is suspended from a steel frame resting on top of the granite block. The major components of the facility include the neutron activation loop and the gamma emission loop. The inlet and outlet of the activation loop are denoted by ‘A’ and ‘B’ respectively, see Fig. 4. Similarly ‘C’ and ‘E’ refer to the inlet and outlet of the decay loop, respectively, see Fig. 5. Point ‘D’ is the front end of the inner coaxial pipe of the decay loop.

was chosen to construct the facility because of its low cost and simple solvent assembly. The geometries of the two loops are described below and the simulated production of  $^{16}\text{N}$  in the neutron activation loop and calculated 6.129 MeV gamma-ray rate from the emission loop are presented in Section 3.

### 2.2. Neutron activation loop

The neutron activation loop, as seen in Fig. 4, consists of 15 m of 4.1 cm (1.5 in. nominal) inside diameter (ID) flexible PVC pipe. This flexible pipe is wrapped around the PNG support structure in two layers with 7 inner layer and 6 outer layer coils. The PNG is



**Fig. 4.** Neutron activation loop consists of 13 coils of flexible PVC pipe wrapped around a steel structure. The steel structure includes a horizontal shelf to position the PNG tube at the center of the activation loop. The red handled valves on the inlet, 'A', and outlet, 'B', of the activation loop are the connections to the supply and return pipes, respectively, as shown in Fig. 3. The arrows indicate the direction of the water flow. (For interpretation of the references to color in this figure legend, the reader is referred to the web version of this article.)

positioned so that the neutron emission plane of symmetry is centered in the activation coil to maximize the production of  $^{16}\text{N}$  across the coil. The volume of the activation loop is  $\sim 22.6$  L. At a flow rate of 2 L/s the water dwells in the region of intense neutron flux of the PNG for  $\sim 9.9$  s. The activated water flows out of the activation loop, labeled 'B' in Fig. 3, through the  $\sim 250$  cm long, 4.1 cm (1.5 in. nominal) ID rigid PVC supply pipe to the input of the gamma emission loop, labeled 'C'.

### 2.3. Gamma emission loop

The gamma emission loop, as seen in Fig. 5, has a coaxial design with a total volume of  $\sim 23.1$  L. The irradiated water flows through the inner, 4.1 cm (1.5 in. nominal) ID, 4.8 cm outside diameter (OD), rigid PVC tube, labeled 'C' in Fig. 3, which ends  $\sim 2$  cm before the inner face of the curved front end cap, labeled 'D'. In this way, the water with the highest level of activation comes out at the front surface of the cylinder, 'D', minimizing the self-attenuation of the water ( $2.77 \times 10^{-2} \text{ cm}^{-1}$  at 6 MeV [10]) and maximizing the gamma-ray flux. The water then flows back through the outer, 20.2 cm (8 in. nominal) ID, clear PVC tube  $\sim 65$  cm long, toward the back end cap and out of the return pipe, labeled 'E'. The increase in pipe cross-sectional area results in a factor of  $\sim 22.9$  slower flow velocity in the outer tube. At a flow rate of 2 L/s, the water dwells in the inner and outer tubes for  $\sim 0.41$  s and  $\sim 9.8$  s respectively. The PVC wye (3 in. nominal ID) at the back of the decay loop provides the coaxial input, 'C', to the gamma decay loop and output, 'D', to the  $\sim 250$  cm long, 4.1 cm (1.5 in. nominal) ID rigid PVC return pipe to the input of the irradiation loop, 'A'. The volume of the supply and return pipes is  $\sim 8.1$  L.

### 3. Simulation results

The water is continuously circulated between the irradiation and decay loops to achieve steady-state gamma-ray emission.



**Fig. 5.** Gamma emission loop consists of two coaxial PVC pipes. The activated water enters through the straight leg of the wye fitting, 'C', and flows through the inner pipe to within 2 cm of the front cap on the left of the emission loop, 'D'. The water flows back through the large diameter tube toward the end cap and out through the angled leg of the wye, 'E', and returns to the irradiation loop. The white handled valves on the straight and angled legs of the wye are the inlet and outlet of the emission loop and the connections to the supply and return pipes, respectively, see Fig. 3. The arrows indicate the direction of the flow.

The activity of the gamma-ray emission loop was simulated as a function of the flow rate to estimate the optimum flow rate and to determine the required capacity of the circulating pump and flow meter. This was done using a two-step simulation process.

#### 3.1. $^{16}\text{N}$ production rate

The production rate of  $^{16}\text{N}$  in the neutron activation loop for the  $^{16}\text{O}(n,p)^{16}\text{N}$  reaction was simulated using Monte Carlo N-Particle eXtended (MCNPX) [11]. The coils of the activation loop surrounding the PNG tube were modeled as a series of water filled PVC tori. The steel structure, granite block and soil were not included in the simulation because only the isotopes of  $^{16}\text{N}$  from the neutron activation loop are transported to the gamma emission loop; the other radiations from the  $^{16}\text{O}(n,p)^{16}\text{N}$  reaction and activation are shielded by the granite block. The simulation model and the probability of  $^{16}\text{N}$  produced per neutron per  $\text{cm}^3$  for each torus estimated by MCNPX can be seen in Fig. 6. The volume weighted average production probability of  $^{16}\text{N}$  across the entire activation loop is  $2.4 \times 10^{-7} \text{ }^{16}\text{N}/\text{n}/\text{cm}^3$ .

The estimated relative error for each measurement point given by MCNP is defined as one standard deviation of the mean divided by the estimated mean [12]. The average relative error is 0.035%, which is too small to be seen in the plot of Fig. 6.

#### 3.2. 6.129 MeV gamma-ray production rate

The activity of the source was estimated as a function of time by solving the following differential equations:

$$\frac{d^{16}\text{N}}{dt} = \sigma\phi^{16}\text{O} - \lambda^{16}\text{N} \quad (1)$$

$$\frac{d^{16}\text{N}}{dt} = -\lambda^{16}\text{N} \quad (2)$$

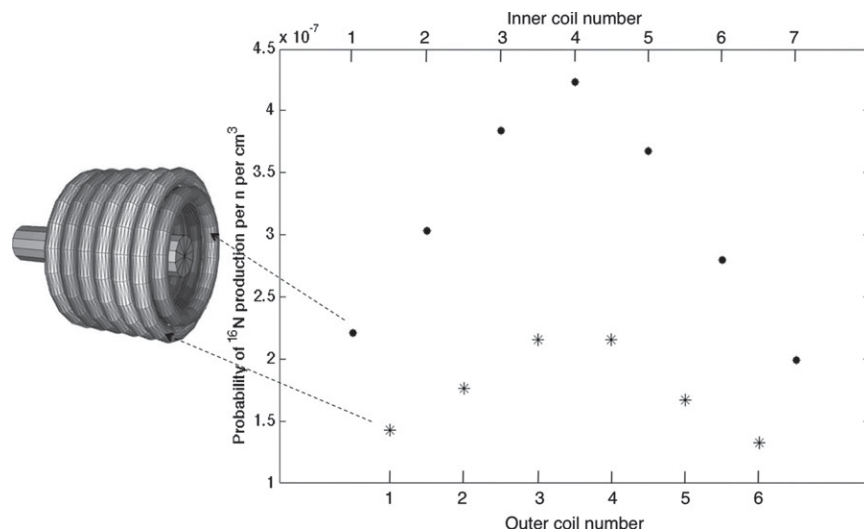


**Fig. 6.**  $^{16}\text{N}$  production in the neutron activation loop was modeled as a nested set of 13 tori (top left), 7 in the inner layer and 6 in the outer layer. The MCNPX simulated probability of  $^{16}\text{N}$  produced per neutron per  $\text{cm}^3$  for each coil of the irradiation loop is plotted. The simulation errors are smaller than the symbols. The volume weighted average value of all 13 tori is  $2.4 \times 10^{-7} \text{ }^{16}\text{N}/\text{n}/\text{s}$ .

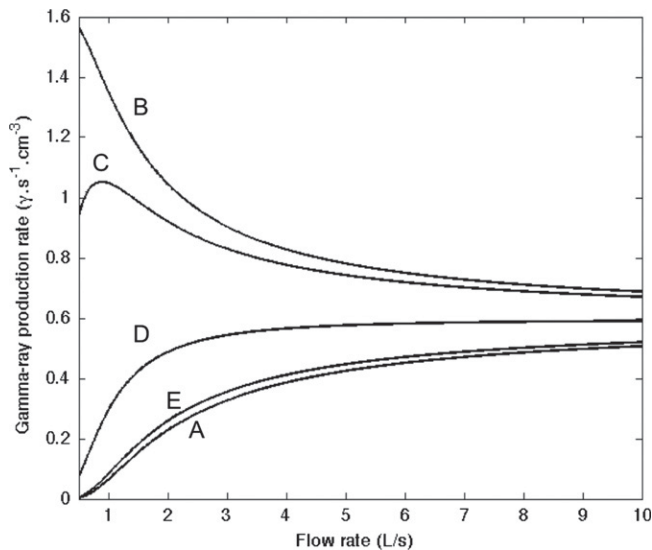


**Fig. 7.** 6.129 MeV gamma-ray production rate calculated as a function of the water flow rate at the beginning, 'A', and end, 'B', of the irradiation loop and at the beginning, 'C', middle, 'D', and end, 'E' of the emission loop, see Fig. 3.

where  $\sigma$  is the cross-section at 14 MeV,  $\phi$  is the neutron flux and  $\lambda$  is the decay constant of the  $^{16}\text{O}(\text{n}, \text{p})^{16}\text{N}$  reaction. Eq. (1) applies to the water circulating in the neutron activation loop and Eq. (2) applies to the water in the decay loop, and the supply and return pipes. The simulated 6.129 MeV gamma-ray flux as a function of the flow rate is shown at different locations in the loop in Fig. 7.

Finally, the steady state activity of the gamma emission loop as a function of the water flow rate was estimated by integrating these results over the volume of the gamma emission loop. Fig. 8 shows the activity of the gamma emission loop as a function of the flow rate on the assumption of a PNG output of  $10^7 \text{ n/s}$  at 14 MeV. The highest flow rate achievable with the Taco 2400-50 circulation pump,  $\sim 2 \text{ L/s}$ , was limited by the head pressure in the plumbing. The stability of the flow rate is very good; the observed variation is less than  $\pm 0.01 \text{ L/s}$  at  $2 \text{ L/s}$ . At this flow rate the 6.129 MeV gamma-ray rate of the gamma emission loop reaches about 85% of its maximum value. A higher flow rate of  $\sim 4 \text{ L/s}$  is

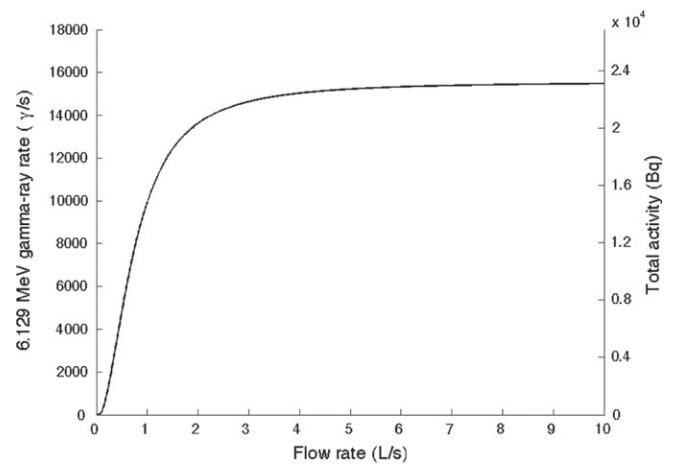


**Fig. 8.** Isotropic 6.129 MeV gamma-ray rate and total isotropic activity of the gamma emission loop as a function of the water flow rate calculated on the assumption of a PNG output of  $10^7 \text{ n/s}$ .

desirable to maximize the gamma-ray flux and to reduce any flux variation on flow rate. This flow rate can be achieved by using a more powerful pump that will be purchased and installed when funding is available.

## 4. Experimental results

### 4.1. Quasi-monoenergetic 6 MeV gamma results

Gamma-ray spectra were acquired with a HPGe detector, Ortec Model GMX30, on the neutron activation loop and gamma emission loop sides of the granite block. The front face of the HPGe detector was placed 10 cm from the forward end of the gamma emission loop and coaxially aligned. With a duty factor of 100%, a voltage of 70 kV and a beam current of  $60 \mu\text{A}$ , the PNG was operated in DC mode, with a constant output of  $\sim 10^7 \text{ n/s}$ . A natural radioactive background spectrum was obtained with the PNG turned-off after waiting for about ten  $^{16}\text{N}$ -beta-decay half-lives ( $\sim 70 \text{ s}$ ) until the short half-life isotopes had decayed. Fig. 9 compares the gamma-ray spectra from the background-subtracted activation loop, emission loop, and  $^{238}\text{Pu}/^{13}\text{C}$  source.

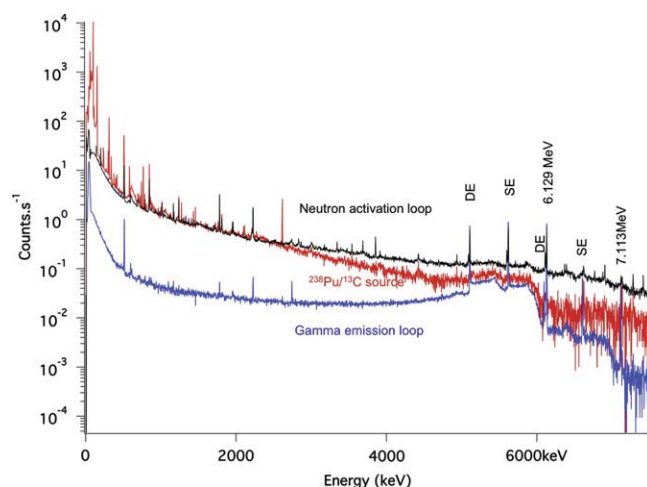


**Fig. 9.** HPGe background subtracted gamma-ray spectra from the neutron activation loop (black), the gamma emission loop (blue) and the  $^{238}\text{Pu}/^{13}\text{C}$  source (red). The spectra of the activation loop and  $^{238}\text{Pu}/^{13}\text{C}$  source have been normalized to match the 6.129 MeV gamma-ray intensity of the gamma emission loop spectrum. (For interpretation of the references to color in this figure legend, the reader is referred to the web version of this article.)

The activation loop and  $^{238}\text{Pu}/^{13}\text{C}$  source spectra were normalized to the 6.129 MeV peak intensity of the emission spectrum in order to compare the low-energy continuum. The reduction in both the gamma-ray continuum and the number of peaks for the gamma emission loop spectrum below  $\sim 5$  MeV and above  $\sim 6$  MeV indicates the shielding effect of the granite block to the gamma rays produced in the granite and soil. The 6.129 MeV and 7.113 MeV photopeaks can be seen along with their single and double escape peaks. The 2.742 MeV photopeak and escape peaks are also visible in the spectra; however, these peaks overlap with the 2.2 MeV and 1.7 MeV neutron capture peaks on H and Si present in the granite, respectively. The 0.511 MeV line is also visible.

#### 4.2. Source activity results

The activity of the gamma emission loop, determined by the integral area under the 6.129 MeV photopeak, was estimated from the experimental data in Fig. 9 using Igor Pro software [13]. The conversion from the HPGe activity to the total activity of the gamma emission loop was determined using MCNP-PoliMi [14] to simulate the gamma-ray interaction probability in the HPGe detector assuming that the number of gamma rays produced by the source is known. The ratio of gamma rays recorded by the HPGe to gamma rays emitted by the gamma emission loop was used with the experimental results to estimate the total activity of the gamma emission loop. The simulation took into account the geometry between the gamma emission loop and HPGe detector, the HPGe efficiency at 6.129 MeV, the gamma-ray attenuation of the water, and the  $^{16}\text{N}$  decay time.

The coaxial design of the gamma emission loop source was simulated as two cylindrical volumes emitting isotropic radiation. The decay time of the  $^{16}\text{N}$  in the water was simulated by setting the source probabilities (SP card in MCNP) as an exponential function on the axial limits of the cylinders. The simulation required the two volumes to be treated separately because of the different flow directions. The results, in units of gamma rays detected in the HPGe per gamma ray emitted, were combined to get the total detection rate, taking into account the difference in flow velocities and volumes of the two cylinders.

The simulation results show that the ratio of gamma rays recorded in the HPGe to gamma rays emitted by the gamma emission loop was  $5.4 \times 10^{-4}$ . The area under the 6.129 MeV photopeak shown in Fig. 9 is  $2.02 \pm 0.01$  gamma rays s/s. The total estimated isotropic gamma-ray rate at 6.129 MeV is  $(3.74 \pm 0.03) \times 10^3$  gammas/s and the total activity of the gamma emission loop is  $(5.42 \pm 0.04) \times 10^3$  Bq.

The difference between the simulated 6.129 MeV gamma-ray rate of  $13 \times 10^3$  gamma/s as seen in Fig. 8 and the experimentally measured activity is attributed to the following.

- Uncertainty in the PNG neutron flux: the PNG neutron yield of  $10^7$  n/s used for the simulation was based on the calibration settings provided by the PNG manufacturer. These settings were also used for operation; however a direct measurement of the PNG neutron flux was not available at the time of this experiment. We plan to purchase a fast neutron monitor, which will provide an accurate measurement of the flux. Based only on the observed gamma-ray flux, the PNG neutron flux was  $\sim 0.4 \times 10^7$  n/s.
- Non-uniform radial velocity profiles in the system: the calculation of 6.129 MeV gamma-ray production rate was made on the assumption of uniform bulk motion of the water,  $1.85 \pm 0.01$  L/s, in the pipes and the neutron activation and gamma emission loops. Our assumption of uniform radial velocity profile in the gamma emission loop would lead to an overestimate of the true gamma-ray flux. A more detailed simulation of the gamma emission loop including the radial dependence of the flow velocity would provide a better estimate of the 6.129 MeV gamma-ray production rate.

#### 5. Conclusion

The 6 MeV Gamma Facility at GSFC provides a quasi-monoenergetic source of 2.742, 6.129 and 7.117 MeV gamma rays suitable for characterization and optimization of a wide range of instruments. Circulation of activated water around a 1.8 m thick granite block reduced the low-energy gamma-ray continuum by a factor of  $\sim 30$  compared to a  $^{238}\text{Pu}/^{13}\text{C}$  source with similar 6.129 MeV gamma-ray rate. Further modifications to the plumbing are expected to increase the flow rate. Future work will also explore the use of oxygen-rich liquids such as ethylene glycol. The 6 MeV Gamma Facility is expected to become a strategic element in the future development of GSFC instruments.

#### Acknowledgment

This work was supported by NASA GSFC Internal Research and Development (IRAD). The authors would like to thank Bert Nahory for assembling the facility, Julia Bodnarik and Robert Forsythe for their help during operations, and Jeffrey Schweitzer and the NASA GSFC neutron/gamma-ray group for their support throughout this work.

#### References

- [1] M. Kroupa, et al., *Journal of Instrumentation* 6 (2011) T11002.
- [2] J.G. Bodnarik, et al. *Proceedings of the 41st Lunar and Planetary Science Conference*, 2010, 2581.
- [3] S.F. Nowicki, S.E. Anderson, A.M. Parsons, *IEEE Nuclear Science. Symposium. Conference. Record*, pp. 4697–4700, 2011.
- [4] N.J. Cherepy, et al., *IEEE Transactions on Nuclear Science (NS)* 56 (2009) 873.
- [5] S.D. Hunter, et al (2012), in: *Proceedings of the SPIE* 8443.
- [6] A. Parsons, J. Bodnarik, L. Evans, S. Floyd, L. Lim, T. McClanahan, M. Namkung, S. Nowicki, J. Schweitzer, R. Starr, J. Trombka, *Nuclear Instrumentation Methods in Physics Research Section A* 652 (2011) 674.

- [7] National Nuclear Data Center, Brookhaven National Laboratory, <<http://www.nndc.bnl.gov>> accessed June 2012.
- [8] G.B. Bishop, Nuclear Instrumentation Methods in Physics Research Section A 121 (1974) 499.
- [9] T. Nishitani, et al., Review of Scientific Instruments 74 (2003) 1735.
- [10] XCOM,; Photon Cross Sections Database, NIST Standard Reference Database 8 (XGAM), <<http://www.nist.gov/pml/data/xcom>> (accessed June 2012).
- [11] D.E., Pelowitz, (Ed.), MCNPX User's Manual, Doc. LA-CP-07-1473, Los Alamos National Laboratory, Los Alamos, NM, 2008.
- [12] X-5 Monte Carlo Team, 2005 (Ed.), MCNP—A General Monte Carlo N-Particle Transport Code, Version 5, Doc. LA-UR-03-1987, Los Alamos National Lab, Los Alamos, NM.
- [13] Igor Pro software v.6.22A, WaveMetrics, Inc., 2010, <<http://www.wavemetrics.com>>.
- [14] E. Padovani, S.A. Pozzi (Eds.), MCNP-PoliMi ver. 1.0 User's Manual, Library of Nuclear Engineering Department Politecnico di Milano Via Ponzio 34/3, 20133 Milano, Italy, Code CESNEF-021125, 2005.